

## Compressive sensing reconstruction of feed-forward connectivity in pulse-coupled nonlinear networks

Victor J. Barranca,<sup>1,\*</sup> Douglas Zhou,<sup>2,†</sup> and David Cai<sup>2,3,4,‡</sup>

<sup>1</sup>*Department of Mathematics and Statistics, Swarthmore College, Swarthmore, Pennsylvania 19081, USA*

<sup>2</sup>*Department of Mathematics, MOE-LSC, Institute of Natural Sciences, Shanghai Jiao Tong University, Shanghai 200240, China*

<sup>3</sup>*Courant Institute of Mathematical Sciences and Center for Neural Science, New York University, New York, New York 10012, USA*

<sup>4</sup>*NYUAD Institute, New York University Abu Dhabi, Abu Dhabi, United Arab Emirates*

(Received 5 September 2015; published 16 June 2016)

Utilizing the sparsity ubiquitous in real-world network connectivity, we develop a theoretical framework for efficiently reconstructing sparse feed-forward connections in a pulse-coupled nonlinear network through its output activities. Using only a small ensemble of random inputs, we solve this inverse problem through the compressive sensing theory based on a hidden linear structure intrinsic to the nonlinear network dynamics. The accuracy of the reconstruction is further verified by the fact that complex inputs can be well recovered using the reconstructed connectivity. We expect this Rapid Communication provides a new perspective for understanding the structure-function relationship as well as compressive sensing principle in nonlinear network dynamics.

DOI: [10.1103/PhysRevE.93.060201](https://doi.org/10.1103/PhysRevE.93.060201)

The structural connectivity in a network is often key to the understanding of its function. However, for many physical systems, e.g., neuronal networks, it is currently infeasible to obtain the full network connectivity due to experimental difficulties [1–7]. Recently, network analysis approaches, such as partial spectral coherence, Granger causality, and dynamic Bayesian network analysis, have been developed in an attempt to reconstruct network connectivity based on measured network outputs [8–12]. However, these methods generally demand long observational data, which severely limit their utility in applications.

Although the connectivity in many biological, social, and technological networks is found to be sparse [13–18], how to reconstruct the connectivity of such networks in general is still a difficult task. *Compressive sensing* (CS) proves to be a useful technique for reconstructing sparse data via very few measurements [19–21] and thus may facilitate connectivity reconstruction using relatively little observational data. Although CS has been applied in recovering the connectivity of many networks [22–25], its application has been restricted to static systems with explicit linear input-output relations. However, many networks possess nonlinear dynamics, and whether CS can be applied to reconstructing their connectivities remains a great theoretical challenge.

In this Rapid Communication, we address under what conditions the CS reconstruction framework can be applied to a general class of pulse-coupled nonlinear networks, i.e., integrate-and-fire (I&F) networks. These network systems emerge from many applications, e.g., gene regulatory modeling, speech recognition, and neuronal dynamics [26–29]. Since the complete structure of the underlying network connectivity usually cannot be obtained, we further address the issue of how to verify the CS reconstructed networks. To answer

these questions so as to deepen the understanding of network structure-function relationships as well as the CS mechanism for sparse signal transmission in nonlinear systems, we develop a theoretical framework for CS reconstruction of sparse feed-forward connectivity of nonlinear I&F networks. First, using nonequilibrium statistical mechanics methods, we reveal a linear mapping between network input and output activity embedded in such nonlinear network dynamics. Then, using a significantly small set of random inputs with short-time duration, we apply CS theory to reconstruct the network connectivity. We further demonstrate that the reconstructed connectivity can be verified by a successful recovery of complex inputs. Our analysis indicates that this reconstruction can even be achieved when the dimension of the network input is significantly greater than the dimension of the measured output. In addition, the recovery of feed-forward connectivity is still possible in the presence of recurrent connections.

We consider the following I&F dynamics with  $m$  nodes and the activity of the  $i$ th node with state variable  $x_i$ ,

$$\tau \frac{dx_i}{dt} = -(x_i - x_R) + \sum_{j=1}^n F_{ij} p_j + \frac{S}{N_R} \sum_{\substack{k=1 \\ k \neq i}}^m R_{ik} \sum_l \delta(t - \tau_{kl}), \quad (1)$$

where the input  $n$ -vector  $\mathbf{p} = (p_j)$  is fed into the network through connections determined by a sparse feed-forward  $m \times n$  matrix  $\mathbf{F} = (F_{ij})$ . Recurrent connections among the nodes are described by an  $m \times m$  matrix  $\mathbf{R} = (R_{ik})$ , where  $S$  is the connection strength and  $N_R$  is the average number of connections per node.  $x_i$  evolves continuously according to Eq. (1) with time-scale  $\tau$  until reaching a threshold value  $x_T$  at which point the node is said to fire and its state is instantaneously reset to the value  $x_R$ . At the moment of the  $l$ th firing event of the  $i$ th node  $\tau_{il}$ , the activity of all neighboring nodes is offset by  $(S/N_R)$ . Integrating over the Dirac  $\delta(\cdot)$  in Eq. (1) takes into account this instantaneous offset at each firing event.

To illustrate the idea of CS reconstruction of sparse feed-forward connectivity, we first consider the network without

\*vbarran1@swarthmore.edu

†zdz@sjtu.edu.cn

‡cai@cims.nyu.edu

recurrent connectivity, i.e.,  $S = 0$ . As typical in experiment, we seek to reconstruct  $\mathbf{F}$  in the case where we only possess information regarding  $r$  inputs, denoted by  $\{\mathbf{p}^{(i)}\}_{i=1}^r$ , and measure the corresponding network output response, i.e., firing rates of network nodes, denoted by  $\{\boldsymbol{\mu}^{(i)}\}_{i=1}^r$ , by accumulating firing events in a short-time duration ( $\sim \tau$ ). Note that  $\boldsymbol{\mu}^{(i)}$  is an  $m$  vector and  $\mathbf{p}^{(i)}$  is an  $n$  vector. For our reconstruction, we use random input for each  $\mathbf{p}^{(i)}$ , i.e., the elements of  $\mathbf{p}^{(i)}$  are chosen as independent uniformly distributed random variables.

Note that the total number of network-output measurements is  $mr$ , whereas the number of unknowns in the feed-forward connectivity is  $mn$ . Here, the experimental constraint is reflected in the fact that  $r$  is much less than  $n$ . Theoretically, to reconstruct the feed-forward connectivity  $\mathbf{F}$  is an underdetermined inverse problem and in general is ill posed. However, since  $\mathbf{F}$  is sparse, i.e., the number of unknowns in  $\mathbf{F}$  is much less than  $mn$ , the recently developed compressive sensing theory might provide a potential tool for such sparse data reconstruction if the dynamics were linear. Here, we however confront a conceptual difficulty because the dynamics of the network system (1) is instead nonlinear.

As outlined in the Appendix, through techniques of nonequilibrium statistical mechanics [30–32], we can coarse grain the nonlinear network dynamics in the relatively high firing-rate regime and obtain an embedded linear mapping between the network inputs  $\mathbf{p}$  and the network output firing rates  $\boldsymbol{\mu}$  as

$$\mathbf{F}\mathbf{p} = \left( \tau\boldsymbol{\mu} + \frac{\mathbf{e}_m}{2} \right) (x_T - x_R), \quad (2)$$

where  $\mathbf{e}_m$  is an  $m$  vector of ones. Note that the firing-rate system (2) was previously derived in the population sense for ensembles of I&F networks with stochastic inputs of homogeneous strength in traditional coarse-graining applications [30–32]. Our work reveals that, over an ensemble of network realizations differing in initial conditions, Eq. (2) is also valid for the case where each network realization is forced by the same set of heterogeneous deterministic inputs.

We are now ready to address the question of whether  $\mathbf{F}$  can be successfully reconstructed using CS based on the linear mapping (2). The theory of CS demonstrates that finite bandwidth signals with a sparse representation may be reconstructed using particularly few measurements of number determined by the signal sparsity rather than the full bandwidth [19,20]. Therefore, for most efficient signal recovery, one should intuitively choose the reconstruction with the most zero components in the sparse domain. Although this optimization problem is generally computationally expensive, it is possible to equivalently reconstruct the sparse representation by instead minimizing the sum of the absolute values ( $L_1$  norm) of the signal components. This  $L_1$  minimization problem can be efficiently solved through numerous algorithms, such as the orthogonal matching pursuit, least absolute shrinkage and selection operator, and the polytope faces pursuit [21,33]. For a large class of measurement matrices with random distributions, CS theory proves that successful reconstruction is achievable in this framework with near certainty [19,20,26–29]. Therefore, recovering the full feed-forward connectivity matrix  $\mathbf{F}$  requires solving a total of  $m$  CS problems. Each corresponds to a distinct row  $\mathbf{F}_{i*}$  for

$i = 1 \cdots m$  using the full set of inputs  $\mathbf{P} = [\mathbf{p}^{(1)} \cdots \mathbf{p}^{(r)}]$  and respective evoked firing rates of node  $i$ ,  $\mathbf{U}_i = [\mu_i^{(1)} \cdots \mu_i^{(r)}]$ . Each CS problem thus has the form

$$\mathbf{F}_{i*}\mathbf{P} = \left( \tau\mathbf{U}_i + \frac{\mathbf{e}_r}{2} \right) (x_T - x_R), \quad (3)$$

where  $\mathbf{F}_{i*}$  is chosen to be the solution to Eq. (3) with a minimal  $L_1$  norm.

To assess the accuracy of the reconstructed connectivity  $\mathbf{F}^{\text{recon}}$ , we measure the relative reconstruction error  $\epsilon = \|\mathbf{F} - \mathbf{F}^{\text{recon}}\| / \|\mathbf{F}\|$  using the Frobenius norm  $\|\mathbf{F}\| = \sqrt{\sum_i \sum_j F_{ij}^2}$ . In Fig. 1(a), we consider a network consisting of  $m = 10^3$  nodes, and the input dimension is  $n = 10^4$ . For simplicity, each feed-forward connection  $F_{ij}$  is chosen as a product between a Bernoulli-distributed random variable with success probability  $p_F = 10^{-3}$  and the input strength  $f$ . As will be discussed below, our results can be naturally extended to alternative sparse feed-forward connectivity with more complex structures, e.g., with local receptive field properties. By using a one order of magnitude smaller number of random inputs, i.e.,  $r = 10^3$ , the relative reconstruction error is  $\sim 12\%$ . In addition, if the feed-forward connection strength is known [34,35], we have verified that the error can be further reduced by thresholding the magnitudes of entries in the reconstructed matrix  $\mathbf{F}^{\text{recon}}$ .

Since an efficient reconstruction of  $\mathbf{F}$  should minimize the number of necessary measurements of network output activity, we plot in Fig. 1(a) the impact of the input ensemble size on the quality of the reconstruction of  $\mathbf{F}$ . It can be seen that the reconstruction error initially rapidly decreases as more inputs are used and then remains nearly constant with further increases in the number of inputs. Therefore, the reconstruction error in this case is already small even using a two orders of magnitude smaller number of inputs, e.g.,  $r = 250$ . Since the measurement of network dynamics may be subject to noise in applications, we also examine the impact of zero-mean Gaussian noise added to the measured firing rates on the reconstruction quality in Fig. 1(b). We observe that there is a nearly linear increase in error with the noise standard deviation after an initial slow rise, yielding accurate reconstructions in the presence of moderate measurement noise.

Considering that the true feed-forward connectivity  $\mathbf{F}$  in general is not available in applications, one encounters an important issue of how to verify the accuracy of  $\mathbf{F}^{\text{recon}}$ . In fact, the linear mapping (2) can provide a methodology to verify the quality of reconstruction by solving another inverse problem, namely, one can apply new inputs  $\mathbf{p}$  and examine whether these new inputs can be well recovered using  $\mathbf{F}^{\text{recon}}$  in combination with the measured network firing rate  $\boldsymbol{\mu}$  in response to these new inputs.

However, this inverse problem may also be ill posed if the number of measurements  $m$  is much less than the input dimension  $n$ . Instead of designing artificial sparse inputs, we can use inputs which are sparse under some linear transformation. Therefore, the effective amount of freedom in  $\mathbf{p}$  is much less than  $n$ , and CS can be applied to reconstruct these inputs. Here, we use visual images as an example of such inputs since it is well known that visual images  $\mathbf{p}^{\text{image}}$  are sparse in the sense that  $\hat{\mathbf{p}} = \mathbf{D}\mathbf{p}^{\text{image}}$ , where the matrix  $\mathbf{D}$  is

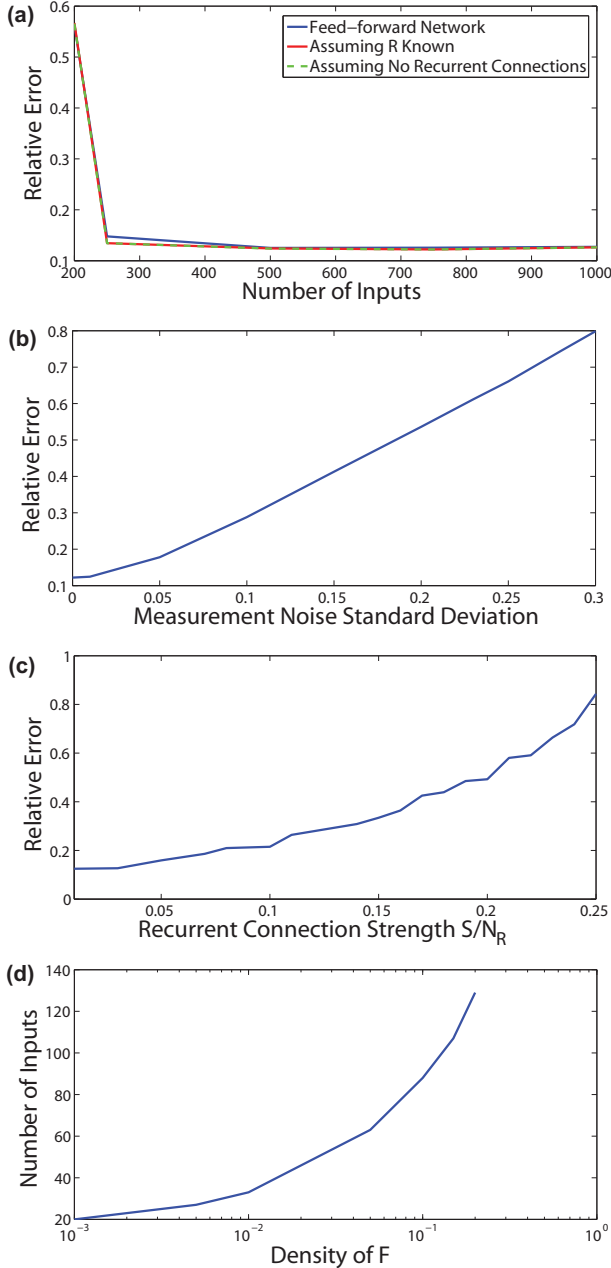


FIG. 1. Relative reconstruction error  $\epsilon$  dependence on input set and matrix density. (a)  $\epsilon$  as a function of the input ensemble size for a feed-forward network (blue) and for a network with recurrent connections that are known (red) or assumed negligible (dashed green). Here,  $m = 10^3$  and  $n = 10^4$ . (b)  $\epsilon$  as a function of the noise (see the text). (c)  $\epsilon$  as a function of recurrent connection strength  $S/N_R$  for a square network of  $m = n = 100$  and  $r = 33$  inputs. (d) Number of inputs required to produce a reconstruction of  $\mathbf{F}$  with  $\epsilon$  less than 0.15 as a function of the connection density of  $\mathbf{F}$ . Network parameters are the same as in (c). In (c) and (d), the error considered is the mean over ten realizations of  $\mathbf{F}$ , exhibiting a small average variance of  $10^{-4}$ . Unless varied, the parameters are chosen as  $S = 1$ ,  $N_R = 0.05m^2$ ,  $\tau = 20$  ms,  $x_R = 0$ ,  $x_T = 1$ ,  $f = \frac{1}{p_F p_c n}$ , and  $p_j \in [0, 255]$ , modeling input pixel intensities. Note characteristic pixel intensity  $p_c = 50$  and  $f$  are chosen such that as the connection density of  $F$  is varied, the feed-forward input into each node remains  $O(1)$ . In (a) and (b), the network-averaged firing rate is approximately 100 Hz.

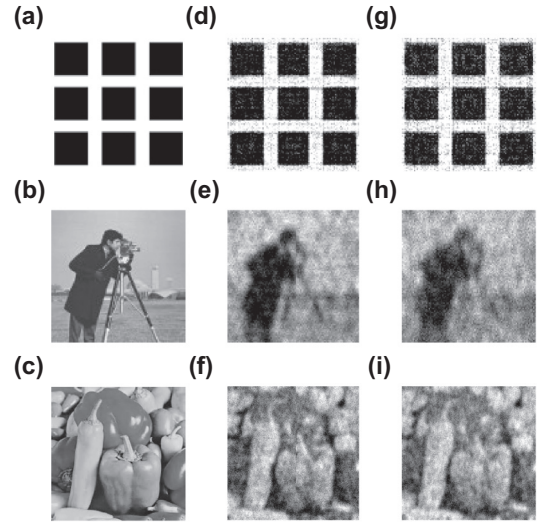


FIG. 2. Input reconstructions using recovered network connectivity. (a)–(c) Input images of size (a) and (b)  $n = 100^2$  and (c)  $n = 250^2$  pixels. (d)–(f) CS reconstructions using the original  $F$ . (g)–(i) CS reconstructions using  $F^{\text{recon}}$ . For images (d)–(f),  $\epsilon$ 's are 0.23, 0.23, and 0.24, respectively. For images (g)–(i),  $\epsilon$ 's are 0.27, 0.27, and 0.22, respectively. Each connection matrix was reconstructed using an ensemble of  $r = 400$  random inputs. For each image, the corresponding downstream network size is  $m = n/10$  with a feed-forward connection density of 0.001.  $\epsilon$  for  $F^{\text{recon}}$  is 14% for the networks corresponding to (a) and (b) and 15% for (c).

a sparsifying transform [19,20,36] and  $\hat{\mathbf{p}}$  is a sparse  $n$  vector. We thus rewrite this inverse problem as

$$\mathbf{F}^{\text{recon}} \mathbf{p}^{\text{image}} = \mathbf{F}^{\text{recon}} \mathbf{D}^{-1} \hat{\mathbf{p}} = \left( \tau \boldsymbol{\mu}^{\text{image}} + \frac{\mathbf{e}_m}{2} \right) (x_T - x_R), \quad (4)$$

where  $\boldsymbol{\mu}^{\text{image}}$  is the network firing-rate vector corresponding to visual image input  $\mathbf{p}^{\text{image}}$ . Using CS based on the linear mapping (4), we recover the sparse representation  $\hat{\mathbf{p}}$ , and, in turn, the original visual image  $\mathbf{p}^{\text{image}}$  even when the dimension of  $\mathbf{p}^{\text{image}}$  is much greater than the number of network-output activity measurements in  $\boldsymbol{\mu}^{\text{image}}$ .

Visual images in Figs. 2(a)–2(c) are inputs into the network of  $m = n/10$  nodes, and the corresponding network firing rates are measured. We first obtain  $\mathbf{F}^{\text{recon}}$  utilizing  $r = 400$  random inputs in the reconstruction as discussed previously. Then, using  $\mathbf{F}^{\text{recon}}$  and the measured network firing rate, we recover each of the respective images as shown in Figs. 2(g)–2(i). It can be seen that the recovered images capture major features of the original visual images. In comparison, Figs. 2(d)–2(f) are recovered images using CS with the original true feed-forward connectivity matrix  $\mathbf{F}$ . We note that there is no significant difference in the reconstruction quality using  $\mathbf{F}^{\text{recon}}$  relative to  $\mathbf{F}$ , indicating a high quality of connectivity reconstruction. As shown in Figs. 2(c), 2(f), and 2(i), the recovery of inputs can be further improved for larger networks. In our simulations, even visual inputs varying in time, such as videos composed of time-evolving image frames, can also be well recovered.

Finally, we investigate the case where the network possesses recurrent connectivity  $\mathbf{R}$  in which the corresponding linear

network input-output relationship is

$$\mathbf{F}\mathbf{p} = \left( \tau\boldsymbol{\mu} + \frac{\mathbf{e}_m}{2} \right) (x_T - x_R) - \frac{S}{N_R} \mathbf{R}\boldsymbol{\mu}. \quad (5)$$

If the recurrent connectivity  $\mathbf{R}$  is also known to be sparse, the CS theory can similarly be applied to reconstruct both  $\mathbf{F}$  and  $\mathbf{R}$  through solving the above inverse problem by measuring the network firing-rate set  $\{\boldsymbol{\mu}^{(i)}\}_{i=1}^r$  corresponding to given input ensemble  $\{\mathbf{p}^{(i)}\}_{i=1}^r$ . In addition, we find that the CS reconstruction performs well when the recurrent connection strength  $S/N_R$  is relatively weak as shown in Fig. 1(a) in which two cases are also presented, i.e., the recurrent connectivity is known, or the recurrent connectivity is neglected. It can be seen that there is only a minor change in the reconstruction error for  $\mathbf{F}$  relative to the fully feed-forward network (no recurrent connectivity). Therefore, the presence of the recurrent connectivity often does not greatly degrade the accuracy of reconstruction. In Fig. 1(c), we depict the reconstruction error dependence on the recurrent connection strength, noting that there is little change in reconstruction quality for small  $S/N_R$  and there is an approximately linear increase in error for larger  $S/N_R$ . Therefore, an accurate reconstruction is not achievable once the drive from neighboring nodes due to strong recurrent connections drowns out the feed-forward input information and thus diminished reconstruction quality of  $F$  is to be expected. In general, CS signal recovery from observed network dynamics is feasible when the network is in an asynchronous regime characterized by relatively uncorrelated firing events [37].

In addition, we investigate the number of inputs sufficient for successful reconstruction as a function of the connection density of  $\mathbf{F}$  as shown in Fig. 1(d). As the connection density of  $\mathbf{F}$  increases and thus more nonzero elements need to be determined, the necessary input ensemble size increases. Once the density of  $\mathbf{F}$  is sufficiently high, we observe a more rapid increase in the number of necessary inputs. This is consistent with the fact that CS is only effective for sparse data reconstruction.

To summarize, we have shown that our framework is useful in reconstructing network wiring diagrams as well as understanding the CS principle in nonlinear network dynamics. Unlike other methods for connectivity reconstruction which rely on learning or specific input design [38,39], our framework utilizes the intrinsic underlying network input-output relationship and does not depend on the input structure. In addition, the connectivity reconstruction can be verified by the recovery of any sparse-signal inputs without the need for comparison with the actual but usually unknown structural connectivity.

Although we have demonstrated that sparse feed-forward connectivity can be reconstructed from measured network activity in response to a relatively small ensemble of inputs for I&F network dynamics, we remark that our framework could be generalized to other network models or experimentally measured networks once an underlying linear input-output relationship can be determined, such as through nonlinear system analysis [40–42]. Both physiological neurons [43,44] and nonlinear neuronal models, such as the quadratic integrate-and-fire, exponential integrate-and-fire, and Hodgkin-Huxley models [28,45,46], are known to have linear input-output

mappings for specific regimes of input strength. Once the dynamics of the nodes are in such a linear regime, our framework could be used to reconstruct the network feed-forward connectivity. Moreover, if the sparse feed-forward connectivity is somewhat structured as in the case of receptive fields in the visual system, CS techniques can be similarly applied and may potentially yield improved reconstructions [47–49].

This work was supported by N.Y.U. Abu Dhabi Institute Grant No. G1301 (V.J.B., D.Z., D.C.), by Grant No. NSFC-91230202, by the Shanghai Rising-Star Program Grant No. 15QA1402600 (D.Z.), Shanghai Grants No. 14JC1403800, No. 15JC1400104, and No. NSFC-31571071, the SJTU-UM Collaborative Research Program (D.C., D.Z.), and by NSF Grant No. DMS-1009575 (D.C.).

## APPENDIX

Seeking a linear input-output mapping, we perform a coarse-graining procedure derived using nonequilibrium statistical mechanics arguments [29,32]. We consider a statistical ensemble of networks, which in general contain both feed-forward and recurrent connections, differing only in the initial state of nodes  $x_j(t=0)$  and resultant input for  $j = 1, \dots, m$ . For each realization of the network in the ensemble, node  $j$  is injected with a new independent spike train of pulses transmitted by neighboring nodes in addition to a constant input current  $(\mathbf{F}\mathbf{p})_j$ . Moreover, the network possesses the same connectivity structure in each realization.

Over the set of all such realizations considered, we analyze the configuration probability  $P_j(x, dx, t)$  of node  $j$  having a state variable inside the infinitesimally small interval  $(x, x + dx)$  at a specific time  $t$ . To compute this probability, we introduce a probability density function  $\rho_j(x, t)$  such that the probability we seek is  $\rho_j(x, t)dx$ . In determining the dynamics of  $P_j(x, dx, t)$ , we consider changes in the configuration probability over a short time interval  $(t, t + dt)$ .

There are two possible changes the configuration probability can undergo, namely (i) smooth and (ii) instantaneous changes. When node  $j$  receives no spikes and is therefore smoothly evolving, its configuration probability will update continuously by Eq. (1) with forcing only from feed-forward input  $(\mathbf{F}\mathbf{p})_j$ . However, the instant node  $j$  receives a spike, its state will jump, thereby instantaneously changing the configuration probability. We group the smooth parts of Eq. (1) into function  $\phi(x)$  and rewrite the dynamics of node  $j$  in the form

$$\frac{dx_j}{dt} = \phi(x_j) + \frac{S}{\tau N_R} \sum_{\substack{k=1 \\ k \neq j}}^m R_{jk} \sum_l \delta(t - \tau_{kl}),$$

where  $\phi(x_j) = \frac{-(x_j - x_R)}{\tau} + \frac{(\mathbf{F}\mathbf{p})_j}{\tau}$ . Hence, for node  $j$ , the smooth change will be

$$[\phi(x)\rho_j(x, t) - \phi(x + dx)\rho_j(x + dx, t)]dt,$$

and the instantaneous change will be

$$\sum_{i \neq j} \mu_i \left[ \rho_j \left( x - \frac{SR_{ji}}{\tau N_R}, t \right) - \rho_j(x, t) \right] dx dt.$$

Therefore, the configuration probability evolves according to

$$\begin{aligned} [\rho_j(x, t + dt) - \rho_j(x, t)]dx &= [\phi(x)\rho_j(x, t) - \phi(x \\ &+ dx)\rho_j(x + dx, t)]dt \\ &+ \sum_{i \neq j} \mu_i \left[ \rho_j \left( x - \frac{SR_{ji}}{\tau N_R}, t \right) - \rho_j(x, t) \right] dx dt. \end{aligned}$$

Taylor expanding to  $O(dx)$  and dividing by the product of differentials  $dx dt$  in the limit as  $dx \rightarrow 0$  and  $dt \rightarrow 0$ , we obtain the Boltzmann equation for  $\rho_j(x, t)$ ,

$$\frac{\partial \rho_j}{\partial t} = -\frac{\partial}{\partial x}(\phi \rho_j) + \sum_{i \neq j} \mu_i \left[ \rho_j \left( x - \frac{SR_{ji}}{\tau N_R}, t \right) - \rho_j(x, t) \right]$$

valid for  $x_R < x < x_T$ . Assuming the jumps in the state variable at firing events are small, considering the elicited magnitude of a postsynaptic potential due to the firing event of a single presynaptic neuron is in general small, we Taylor expand in  $\frac{SR_{ji}}{\tau N_R}$  to  $O[(\frac{SR_{ji}}{\tau N_R})^2]$ , obtaining the Fokker-Planck equation,

$$\frac{\partial \rho_j}{\partial t} = \frac{\partial}{\partial x} \left( (x - x_R)/\tau \rho_j - g_j \rho_j + \sigma_j^2 \frac{\partial \rho_j}{\partial x} \right),$$

where

$$g_j = \sum_{i \neq j} \mu_i \frac{SR_{ji}}{\tau N_R} + \frac{(\mathbf{Fp})_j}{\tau}$$

is the mean input injected into node  $j$  and

$$\sigma_j^2 = \frac{SR_{ji}}{\tau N_R} \left( \frac{SR_{ji} \mu_i}{2\tau N_R} \right)$$

is the variance in the input fluctuations of node  $j$ .

The Fokker-Planck equation may be expressed in terms of the probability flux  $-J_j$  of the state variable in conservation form

$$\frac{\partial \rho_j}{\partial t} + \frac{\partial J_j}{\partial x} = 0.$$

To derive boundary conditions, we note that, when the state variable of a node reaches threshold  $x_T$ , we instantaneously reset the state variable to  $x_R$ . Thus, the state variable flux at  $x = x_T$  and  $x = x_R$  must be identical. Furthermore, assuming node  $j$  has a firing rate of  $\mu_j$ , the equality of flux across the boundary requires  $J_j(x = x_T) = J_j(x = x_R) = \mu_j$ .

To conclude the coarse graining, we analyze the Fokker-Planck equation in the *mean-driven* operating regime. This means that  $\sigma_j^2$  vanishes, and we obtain the reduced partial differential equation,

$$\frac{\partial \rho_j}{\partial t} = \frac{\partial}{\partial x} \left( \frac{(x - x_R)}{\tau} \rho_j - g_j \rho_j \right).$$

Assuming the firing rates and corresponding configuration probability density function reach a temporal steady state in which  $\frac{\partial \rho_j}{\partial t} = 0$ , the Fokker-Planck equation is reduced to the ordinary differential equation,

$$\frac{\partial}{\partial x} \left( \frac{(x - x_R)}{\tau} \rho_j - g_j \rho_j \right) = -\frac{\partial J_j}{\partial x} = 0,$$

which can be solved exactly for  $\rho_j$  with

$$\rho_j = \frac{\tau \mu_j}{\tau g_j - (x - x_R)}.$$

Since  $\rho_j$  is a probability density function over domain  $[x_R, x_T]$ , it must satisfy the normalization condition  $\int_{x_R}^{x_T} \rho_j(x) dx = 1$ , and therefore we obtain the implicit definition for the firing rate,

$$1 = (\tau \mu_j) \ln \left( \frac{\tau g_j}{\tau g_j - (x_T - x_R)} \right).$$

The drive from the feed-forward input  $(\mathbf{Fp})_j$  can then be explicitly solved for yielding

$$(\mathbf{Fp})_j = \frac{(x_T - x_R)}{1 - \exp\left(\frac{-1}{\tau \mu_j}\right)} - \frac{S}{N_R} (\mathbf{R}\boldsymbol{\mu})_j.$$

Assuming the feed-forward input into each node is relatively large, the number of firing events for each node within time scale  $\tau$  is  $O(1)$ . Under this assumption, we Taylor expand about small parameter  $\frac{1}{\tau \mu_j}$  to  $O(\frac{1}{\tau \mu_j})$  and obtain

$$(\mathbf{Fp})_j = \tau \mu_j (x_T - x_R) + \frac{(x_T - x_R)}{2} - \frac{S}{N_R} (\mathbf{R}\boldsymbol{\mu})_j.$$

The above equation can be written in vector form, yielding the linear input-output mapping (2) in the absence of recurrent connectivity and linear mapping (5) in the presence of recurrent connectivity.

- 
- [1] S. Strogatz, *Nature (London)* **410**, 268 (2001).  
 [2] S. Boccaletti, V. Latora, Y. Moreno, M. Chavez, and D.-U. Hwang, *Phys. Rep.* **424**, 175 (2006).  
 [3] T. S. Gardner, D. di Bernardo, D. Lorenz, and J. J. Collins, *Science* **301**, 102 (2003).  
 [4] I. H. Stevenson, J. M. Rebesco, L. E. Miller, and K. P. Kording, *Curr. Opin. Neurobiol.* **18**, 582 (2008).  
 [5] M. Gomez-Rodriguez, J. Leskovec, and A. Krause, *T. Knowl. Discov. D* **5**, 21 (2012).  
 [6] N. Eagle, A. S. Pentland, and D. Lazer, *Proc. Natl. Acad. Sci. USA* **106**, 15274 (2009).  
 [7] S. Song, P. J. Sjöström, M. Reigl, S. Nelson, and D. B. Chklovskii, *PLoS Biol.* **3**, e68 (2005).  
 [8] D. Zhou, Y. Xiao, Y. Zhang, Z. Xu, and D. Cai, *Phys. Rev. Lett.* **111**, 054102 (2013).  
 [9] S. Eldawlatly, Y. Zhou, R. Jin, and K. G. Oweiss, *Neural Comput.* **22**, 158 (2010).  
 [10] R. Dahlhaus, M. Eichler, and J. Sandkuhler, *J. Neurosci. Methods* **77**, 93 (1997).  
 [11] Y. Hata, T. Tsumoto, H. Sato, and H. Tamura, *J. Physiol. (London)* **441**, 593 (1991).  
 [12] M. Timme, *Phys. Rev. Lett.* **98**, 224101 (2007).

- [13] A. Barabasi and R. Albert, *Science* **286**, 509 (1999).
- [14] D. J. Watts and S. H. Strogatz, *Nature (London)* **393**, 440 (1998).
- [15] Y. He, Z. J. Chen, and A. C. Evans, *Cereb. Cortex* **17**, 2407 (2007).
- [16] S. Achard and E. Bullmore, *PLoS Comput. Biol.* **3**, e17 (2007).
- [17] H. Markram, J. Lubke, M. Frotscher, A. Roth, and B. Sakmann, *J. Physiol.* **500**, 409 (1997).
- [18] A. Mason, A. Nicoll, and K. Stratford, *J. Neurosci.* **11**, 72 (1991).
- [19] E. J. Candes, J. K. Romberg, and T. Tao, *Commun. Pure Appl. Math.* **59**, 1207 (2006).
- [20] D. L. Donoho, *IEEE Trans. Inform. Theory* **52**, 1289 (2006).
- [21] J. A. Tropp and A. C. Gilbert, *IEEE Trans. Inform. Theory* **53**, 4655 (2007).
- [22] A. Emad and O. Milenkovic, *PLoS One* **9**, e90781 (2014).
- [23] A. Noor, E. Serpedin, M. Nounou, and H. Nounou, *Adv. Bioinform.* **2013**, 205763 (2013).
- [24] W.-X. Wang, Y.-C. Lai, C. Grebogi, and J. Ye, *Phys. Rev. X* **1**, 021021 (2011).
- [25] Y. Mishchenko and L. Paninski, *J. Comput. Neurosci.* **33**, 371 (2012).
- [26] A. Corral, C. J. Pérez, A. Díaz-Guilera, and A. Arenas, *Phys. Rev. Lett.* **74**, 118 (1995).
- [27] W. Mather, M. R. Bennett, J. Hastay, and L. S. Tsimring, *Phys. Rev. Lett.* **102**, 068105 (2009).
- [28] V. J. Barranca, D. C. Johnson, J. L. Moyher, J. P. Sauppe, M. S. Shkarayev, G. Kovačič, and D. Cai, *J. Comput. Neurosci.* **37**, 161 (2014).
- [29] A. V. Rangan and D. Cai, *Phys. Rev. Lett.* **96**, 178101 (2006).
- [30] A. Treves, *Network* **4**, 259 (1993).
- [31] R. Ben-Yishai, R. Bar-Or, and H. Sompolinsky, *Proc. Natl. Acad. Sci. USA* **92**, 3844 (1995).
- [32] D. Cai, L. Tao, M. Shelley, and D. McLaughlin, *Proc. Natl. Acad. Sci. USA* **101**, 7757 (2004).
- [33] D. L. Donoho and Y. Tsaig, *IEEE Trans. Inform. Theory* **54**, 4789 (2008).
- [34] B. Barbour, N. Brunel, V. Hakim, and J. P. Nadal, *Trends Neurosci.* **30**, 622 (2007).
- [35] N. T. Markov, P. Misery, A. Falchier, C. Lamy, J. Vezoli, R. Quilodran, M. A. Gariel, P. Giroud, M. Ercsey-Ravasz, L. J. Pilaz, C. Huissoud, P. Barone, C. Dehay, Z. Toroczkai, D. C. Van Essen, H. Kennedy, and K. Knoblauch, *Cereb. Cortex* **21**, 1254 (2011).
- [36] E. J. Candes and M. B. Wakin, *IEEE Signal Process Mag.* **25**, 21 (2008).
- [37] V. J. Barranca, G. Kovačič, D. Zhou, and D. Cai, *Phys. Rev. E* **90**, 042908 (2014).
- [38] G. Isley, C. J. Hillar, and F. T. Sommer, *NIPS* (Curran Associates, Inc., Vancouver, Canada, 2010), p. 910.
- [39] S. Ganguli and H. Sompolinsky, *Annu. Rev. Neurosci.* **35**, 485 (2012).
- [40] N. Wiener, *Nonlinear Problems in Random Theory*, Technology Press Research Monographs (The Technology Press of Massachusetts Institute of Technology and John Wiley & Sons, Cambridge, MA, 1958).
- [41] J. Victor, in *Nonlinear Vision: Determination of Neural Receptive Fields, Function, and Networks*, edited by B. N. R.B. Pinter (CRC, Boca Raton, FL, 1992), p. 1.
- [42] R. A. Silver, *Nat. Rev. Neurosci.* **11**, 474 (2010).
- [43] A. Rauch, G. La Camera, H.-R. Luscher, W. Senn, and S. Fusi, *J. Neurophysiol.* **90**, 1598 (2003).
- [44] G. La Camera, A. Rauch, D. Thurbon, H. R. Luscher, W. Senn, and S. Fusi, *J. Neurophysiol.* **96**, 3448 (2006).
- [45] N. Brunel and P. Latham, *Neural Comp.* **15**, 2281 (2003).
- [46] N. Fourcaud-Trocme and N. Brunel, *J. Comput. Neurosci.* **18**, 311 (2005).
- [47] B. A. Olshausen and D. J. Field, *Network* **7**, 333 (1996).
- [48] B. A. Olshausen and D. J. Field, *Vision Res.* **37**, 3311 (1997).
- [49] V. J. Barranca, G. Kovačič, D. Zhou, and D. Cai, *PLoS Comput. Biol.* **10**, e1003793 (2014).